Click Here for Full Article

Clustering of eastern North Pacific tropical cyclone tracks: ENSO and MJO effects

Suzana J. Camargo

International Research Institute for Climate and Society, Earth Institute at Columbia University, Palisades, New York 10964, USA

Now at Lamont–Doherty Earth Observatory, Earth Institute at Columbia University, Palisades, New York 10964, USA (suzana@ldeo.columbia.edu)

Andrew W. Robertson and Anthony G. Barnston

International Research Institute for Climate and Society, Earth Institute at Columbia University, Palisades, New York 10964, USA

Michael Ghil

Department of Atmospheric and Oceanic Sciences and Institute for Geophysics and Planetary Physics, University of California, Los Angeles, California 90095, USA

Also at Département Terre-Atmosphère-Océan and Laboratoire de Météorologie Dynamique, CNRS/IPSL, Ecole Normale Supérieure, F-75231 Paris, France

[1] A probabilistic clustering technique is used to describe tropical cyclone tracks in the eastern North Pacific, on the basis of their shape and location. The best track data set is decomposed in terms of three clusters; these clusters are analyzed in terms of genesis location, trajectory, landfall, intensity, seasonality, and their relationships with the El Niño–Southern Oscillation (ENSO) and Madden-Julian Oscillation (MJO). Longitudinal track location plays a strong discriminating role in the regression mixture model's solution, with the average track orientation becoming more zonal toward the west. This progression encapsulates well the relationship between tropical cyclones over the eastern tropical Pacific and the MJO or ENSO. Two of the clusters describe tropical cyclones (TCs) with tracks that lie near the coast of Mexico and Central America. The most frequent cluster contains tracks that trend west-northwestward, while the second most frequent one has genesis locations that lie slightly to the southeast of those in the most frequent cluster and tracks that run typically parallel to the Central American coast. This second cluster is shown to be significantly associated with the westerly phase of the MJO. The third, least frequent cluster contains TCs with westward trajectories over the central and eastern equatorial Pacific; some of these TCs have an impact on Hawaii and other islands, as far as the central and western North Pacific regions. The least frequent cluster is strongly related to ENSO, while the others are not; it occurs significantly more frequently during El Niño conditions. Examination of the large-scale patterns of atmospheric circulation and sea surface temperature associated with each of our three clusters are consistent with previous studies. Anomalous low-level westerly zonal winds from the monsoon trough and MJO meet anomalous easterlies near the region of genesis in each cluster.

Components: 10,399 words, 17 figures, 3 tables.

Keywords: hurricanes; eastern North Pacific; tropical cyclones; cluster analysis; ENSO; MJO.

1. Introduction

[2] The eastern North Pacific (ENP) exhibits a high level of tropical cyclone (TC) activity. The most typical TC trajectory in the ENP basin is oriented toward west-by-northwest, leading to TCs that in most cases do not affect land. Nonetheless, the western Mexican coast suffers the impact of many TCs, which either make landfall or move along Mexican coastal waters parallel to the coastline. The main impacts of the TCs in Mexico are associated with high rainfall that occurs when the TCs interact with Mexican mountains [*Jáuregui*, 2003; *Romero-Vadillo et al.*, 2007]. Pacific TCs are an important source of precipitation in southwestern North America [*Englehart and Douglas*, 2001]. They are related to gulf surge events, which influence precipitation in Mexico and southwestern U.S. states, such as Arizona and New Mexico [*Higgins and Shi*, 2005].

[3] TC activity in various ocean basins is strongly influenced by ENSO (El Niño Southern Oscillation). This topic has been studied in many papers and summarized in reviews by *Landsea* [2000] and *Chu* [2004]. The nature of impact of ENSO on TC activity varies from region to region. In the Atlantic, for instance, the number of TCs is usually below normal during an El Niño year [e.g., *Gray*, 1984; *Gray and Sheaffer*, 1991; *Gray et al.*, 1993; *Knaff*, 1997], with an above-normal number of TCs in La Niña years. ENSO also impacts hurricane intensity [*Landsea et al.*, 1999], genesis location [*Elsner and Kara*, 1999] and landfall probabilities in the U.S. and Caribbean [*O'Brien et al.*, 1996; *Bove et al.*, 1998; *Pielke and Landsea*, 1999; *Tartaglione et al.*, 2003; *Smith et al.*, 2007].

[4] ENSO impacts have primarily been studied in terms of the impacts on particular TC statistics, especially the number of TCs (NTCs), but also their intensity, genesis location and landfall probability. With the exception of intensity, these statistics can be derived from the tracks of TCs, which potentially also contain much additional information such as shape, length, velocity, and lifetime.

Through probabilistic models that describe the trajectories of TCs, it may be possible to develop probabilistic predictions of damage-causing potential, together with a more complete picture of their relationships with ENSO and the Madden-Julian Oscillation (MJO).

[5] In a recent two-part paper, *Camargo et al.* [2007c, 2007d], a mixture of regression models was used to describe the shapes and locations of historical TC tracks over the western North Pacific, and to study the impact of ENSO. The regression mixture model provides a principled probabilistic partitioning of the set of best track trajectories into a small set of clusters, based on their shape and location. Previous studies had already shown a shift of the typhoon genesis location, with a southeastward shift of the mean genesis location in El Niño years [*Chan*, 1995; *Chia and Ropelewski*, 2002], and related changes in lifetime and intensity in ENSO years [*Wang and Chan*, 2002; *Camargo and Sobel*, 2005]. By partitioning the best track data set into a set of clusters based on track shape and location, it was shown that certain track types are more common during El Niño events, while others occur more often in La Niña events, with some track types being unrelated to ENSO.

[6] The regression mixture model also provides a dynamical systems perspective in which each cluster reflects more frequently recurring or persistent configurations of TC behavior as characterized by trajectories of a given shape and location. The fluctuation-dissipation theorem of statistical mechanics relates the mean response to impulsive external forcing of a dynamical system to its natural unforced variability [*Leith*, 1975]. To the extent that the clusters tend to reflect the latter, the response to ENSO (or MJO) forcing would tend to be reflected in changes in the prevalence of each cluster.

[7] In this study, we exploit this perspective to gain insight into the relationship between track types and ENSO and MJO. The track types that are influenced by ENSO and MJO are expected to have a greater level of predictability on seasonal

and intraseasonal timescales, respectively, than other track types. In the future, these relationships could be built upon to develop probabilistic predictions of TCs in the ENP at seasonal and intraseasonal lead times.

[8] Here, we present our analysis in two steps. First, we apply the cluster analysis to the TC tracks and analyze the main characteristics of each cluster. Then, relationships with ENSO and the MJO are investigated. Our principal finding is that the regression model-based clustering provides a parsimonious description of TC activity in the ENP basin, bringing together the main attributes seen in previous studies. In particular, we show that a three-cluster solution delineates TCs that are significantly associated with El Niño and the MJO.

[9] A survey of previous studies of tropical cyclone activity in the ENP is provided in section 2, which forms the background for the present study. The cluster analysis and data are briefly described in section 3. The cluster analysis results for ENP tracks are discussed in section 4; the relationship between Pacific hurricanes and ENSO and MJO is examined in section 5 and the large-scale composites of each cluster are shown in section 6. The conclusions are given in section 7.

2. Background on Eastern North Pacific TCs

2.1. Attributes, Cyclogenesis, and Relationships with MJO

[10] The ENP basin is defined as the region between 140°W and the Pacific American coast. A recent discussion of the statistics of TCs in this region is given by Romero-Vadillo et al. [2007]. In this study, we consider all TCs with tropical storm intensity or higher that are active within this region, including TCs that form west of the 140°W (Central North Pacific), but are included in the best track data set from the National Hurricane Center.

[11] The main genesis region in the ENP is the area west of the Gulf of Tehuantepec, between 8 and 15°N, with a mean of 16.3 named TCs per year in the period 1970–2006. The typical hurricane season occurs from May to November, with a peak from July to September. The most typical movement is toward west-by-northwest trajectory, with some having a recurving trajectory turning to the northeast. It is rare that Pacific TCs reach north of 30°N [Romero-Vadillo et al., 2007].

[12] Sánson [2004] discussed the possible influence of topography in the tracks of ENP hurricanes in idealized simulations, depending on the geographical position with respect to the continental mountains and TC intensity. Their study suggests that intense vortices near the continent tend to drift along the coast, trapped by the coastal mountains.

[13] A high percentage of ENP hurricanes impact western Mexico, making landfall in Mexican territory or affecting Mexican coastal waters. The main impact of these TCs in Mexico involves extreme rainfall events, when TCs interact with the mountain ranges of the Sierra Madre and can lead to flooding. The Mexican region most vulnerable to hurricanes is in the northwest of the country (Sinaloa and southern part of Baja California peninsula) [Jáuregui, 2003].

[14] The ENP is the most active region of tropical cyclogenesis globally in terms of genesis per unit area and unit time [Molinari et al., 2000]. Tropical cyclogenesis in the ENP often occurs in association with easterly waves, many being generated in Africa [Avila, 1991; Avila and Pasch, 1992]. However, because of the impacts of other governing factors, the amplitude of these easterly waves is only weakly correlated with tropical cyclogenesis in the ENP. The active and inactive periods of cyclogenesis in the ENP are strongly controlled by the MJO [Molinari et al., 1997; Maloney and Hartmann, 2000, 2001]. More than twice as many TCs occur in the westerly MJO phase than in the easterly phase [Maloney and Hartmann, 2000].

[15] Many other factors are considered to influence the cyclogenesis in the region, such as Central America mountain influences, wind surges, and various mesoscale processes [e.g., McBride and Zehr, 1981; Zehnder, 1991; Zehr, 1992; Bister and Emanuel, 1997; Ferreira and Schubert, 1997]. Molinari and Vollaro [2000] proposed a combination of all these factors, with strong easterly waves crossing the Central America mountains, and then encountering favorable environmental conditions (warm sea surface temperatures, low vertical shear). In particular, the presence of easterlies meeting low-level monsoon westerlies enhances the likelihood of cyclogenesis in the ENP. The importance of the southwesterly monsoon flow for intense ENP hurricanes was also shown using composites [Vincent and Fink, 2001].

[16] Annular hurricanes (distinctively axisymmetric hurricanes with circular eyes surrounded by a nearly uniform ring of deep convection) occur

systematically in the ENP region. These annular hurricanes maintain their intensities longer than the average hurricane and represent a challenge for intensity forecasts [*Knaff et al.*, 2003].

[17] *Whitney and Hobgood* [1997] noticed that storms west of 110°W exhibit a higher average relative intensity than systems farther to the east. As the TCs develop in the ENP basin, the planetary vorticity gradient and the steering winds tend to move these storms to the north and west while they intensify. The combination of increased vertical shear and interaction with land produces lower relative intensity in the storms east of 110°W.

2.2. Relationships With ENSO

[18] In the ENP region, ENSO has been found not to affect the TC frequency [*Whitney and Hobgood*, 1997], but the number of intense hurricanes tends to increase during El Niño years [*Gray and Sheaffer*, 1991]. *Elsner and Kara* [1999] noticed the existence of a see-saw of TC activity between the Atlantic and ENP, with enhanced TC activity in the ENP when the Atlantic is suppressed and vice versa. The genesis location in the ENP tends to shift westward in El Niño events [*Irwin and Davis*, 1999; *Kimberlain*, 1999; *Chu and Zhao*, 2007], and there are more hurricanes that propagate to the central North Pacific [*Chu*, 2004].

[19] *Irwin and Davis* [1999] examined the relationship of the ENP TC tracks and ENSO, but using a very different technique than the one used here. In the work by *Irwin and Davis* [1999] the TCs were stratified into three groups according to the value of the Southern Oscillation Index (SOI). The mean origin and downgrading (dissipation) location of the TCs in El Niño years was found to be west of the mean longitudes for the neutral and La Niña groups. Also, in neutral and La Niña years the ending positions of the ENP tracks were observed to be somewhat more northerly than in El Niño years.

[20] In El Niño years, although the storms reach their maximum intensity at more southwest positions than in neutral or La Niña years, there seems to be little difference in the maximum intensities and relative intensities in association with the ENSO condition [*Whitney and Hobgood*, 1997]. The shift in the location of the storms' maximum intensity is associated with differences in the atmospheric flow in El Niño years, rather than in the pattern of SST anomalies [*Whitney and Hobgood*, 1997].

[21] Changes of TC activity in the ENP and Atlantic basins are associated with anomalies in the large-scale atmospheric and oceanic variables in ENSO events. *Shapiro* [1987] and *Goldenberg and Shapiro* [1996] related the suppressed TC activity in the Atlantic to an increase in the vertical wind shear in that region, while *Tang and Neelin* [2004] stressed the importance of thermodynamic factors.

[22] In the ENP, *Collins and Mason* [2000] identified differing environmental parameters affecting TC activity for the regions east versus west of 116°W. *Collins and Mason* [2000] observed that in the eastern part of the region, the environmental parameters are nearly always at levels conducive to TC formation during the peak season, while in the western region, there are some years when the parameters are conducive to cyclogenesis but other years when they are less so. Using genesis potential index anomaly composites keyed to the ENSO condition, *Camargo et al.* [2007b] concluded that in the eastern North Pacific, wind shear is the main contributor to ENSO-based genesis potential anomalies, with potential intensity [*Emanuel*, 1988] also playing a role.

2.3. Longer Timescales

[23] *Zhao and Chu* [2006] performed a Bayesian multiple change point analysis of hurricane activity in the ENP for the period 1972–2003. Their results indicate that the ENP hurricane activity has a decadal variability with two change points (1982 and 1999), with inactive eras in the periods 1972–1981 and 1999–2003 and an active epoch during 1982–1998.

3. Data and Methodology

[24] The TC data used in this paper is the National Hurricane Center best track data for ENP tropical cyclones (available online at http://www.nhc.noaa.gov/). The best track data set for the ENP is available for the years 1949–2006. The full data set is used to determine the cluster types. Only TCs that have at least tropical storm intensity are used in our analysis; that is, tropical depressions are not included. Here we include all TCs with tropical storm intensity or higher that are in the data set, independent of the point of origin.

[25] The ENSO indices used here are from the Climate Prediction Center (available online at http://www.cpc.ncep.noaa.gov/data/indices/) and

are defined from 1950 to 2006. Therefore, we used this slightly shorter period in our composites.

[26] The composites used different data sources, and the composites used the maximum number of years available for each data. The atmospheric wind composites were obtained using the NCEP/ NCAR reanalysis [*Kalnay et al.*, 1996]. The *Liebmann et al.* [1994] outgoing long-wave radiation (OLR) data set was used, available in the period 1974–2006. We used weekly sea surface temperature (SST) data available from November 1981 to the present [*Reynolds et al.*, 2002].

[27] Only a very brief summary of the clustering technique is given here. A detailed description is given by *Gaffney et al.* [2007], with an application to Atlantic extratropical cyclones. A complete analysis of its application to typhoon tracks is given by *Camargo et al.* [2007c, 2007d]. (A Matlab toolbox with the clustering algorithms described in this paper is available at http:// www.datalab.uci.edu/resources/CCT/.)

[28] The technique consists of building a mixture of polynomial regression models (i.e., curves), which are used to fit the geographical "shape" of the trajectories [*Gaffney et al.*, 2007]. This technique is an extension of the standard finite mixture model to allow for the representations of a mixture of underlying functions (in this case, quadratics), from which the observed TC tracks might have been generated. Finite mixture models enable highly non-Gaussian probability density functions, whether multimodal or not, to be expressed as a mixture of a few unimodal component probability distribution functions. The model is fit to the data by maximizing the likelihood of the parameters, given the data set. As in the work by *Camargo et al.* [2007c, 2007d], the initial TC position is retained in the analysis, so that the clustering considers both the shape as well as the geographical position of each TC. The mixture model framework allows the clustering problem to be posed in a probabilistic context, and to easily accommodate TC tracks of different lengths, contrasting with the K means method used in other studies [e.g., *Harr and Elsberry*, 1995; *Elsner*, 2003; *Elsner and Liu*, 2003]. Each TC is assumed to be generated by one of K different regression models, and each model has its own "shape" parameters consisting of regression coefficients and noise matrix; the latter describes the variances in longitude and latitude of each observed TC position given the model, with the cross-covariance terms set to zero. Detailed discussion of the cluster

methodology, its advantages and examples are given by *Gaffney et al.* [2007].

3.1. Number of Clusters

[29] As is common in cluster analysis, the choice of the number of clusters to be used is not uniquely determined. As a first choice, we used in-sample log-likelihood values, similar to *Camargo et al.* [2007d], to evaluate the possible optimal choice for the number of clusters. The log-likelihood is defined as the log-probability of the observed data under the model, and can be interpreted as a goodness-of-fit metric for probabilistic models. The best possible choice for the number of clusters is the one with the largest log-likelihood value. Figure 1a shows the in-sample log-likelihood values for each cluster number. The log-likelihood values increase in direct relation to the number of clusters n, with the curve flattening for $n >= 5$. Therefore the log-likelihood does not directly provide an optimal number of clusters. A similar behavior was noted by *Camargo et al.* [2007d] who also found the out-of-sample log-likelihood curve to be similar to the one calculated in-sample. Another measure to evaluate the number of clusters is the within-cluster spread, shown in Figure 1b. The spread values were obtained by calculating the difference in latitude and longitude from the mean regression track, squaring, and summing over all the TCs in each cluster. Similarly to the log-likelihood curve, there is no direct indication of an optimal number of clusters, as the spread diminishes as the number of clusters decreases. However, in both curves an obvious diminishing improvement in fit for $n >= 5$ is clear, suggesting a reasonable range of choices of cluster number to be between $n = 3–5$.

[30] We also carried out a qualitative analysis based on how much the track types differ from one cluster to another as the number of cluster increases. The main difference in adding another cluster is that the track types that form farther from the American continent are split into more clusters, with formation locations farther to the west of the continent (Figure 2). Another consideration is that in order to have meaningful and statistically significant composites, a reasonable number of TCs should be present in each cluster. As the cluster that is being subdivided according to different formation locations is the cluster with fewer TCs, as will be shown later, by increasing the number of clusters, the statistical significance of that type of cluster will be compromised as it is further subdivided.
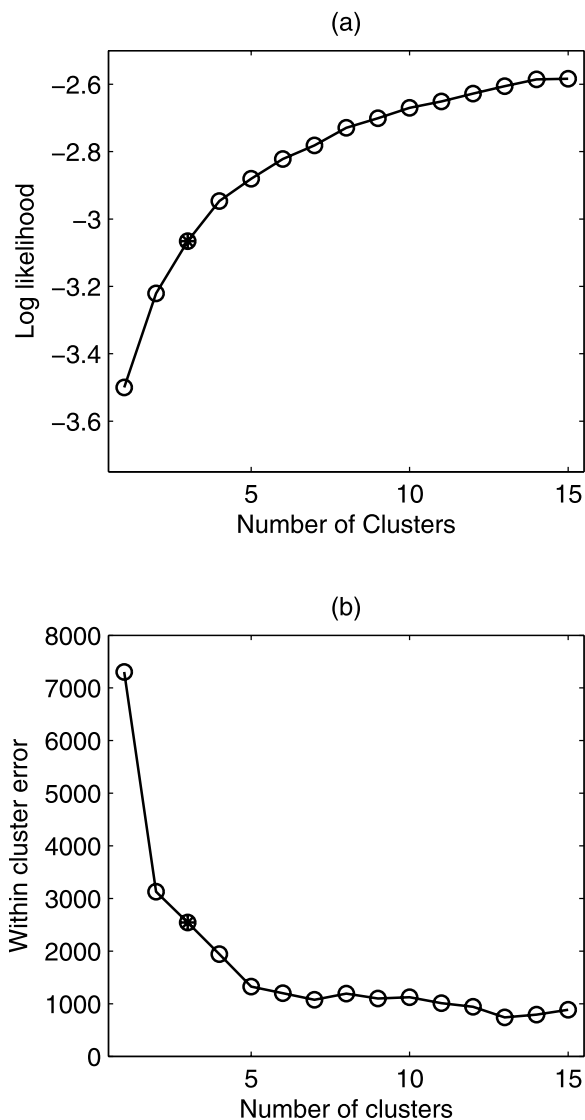
Figure 1. (a) Maximum log-likelihood values for different number of cluster numbers. (b) Minimum within-cluster spread for different number of cluster numbers. The log-likelihood and spread values shown are the maximum and minimum, respectively, of 20 integrations, of the cluster model from different initial seeds.

of tropical cyclones (NTC), and of Accumulated Cyclone Energy (ACE [*Bell et al.*, 2000]), with the Nino3.4 SST index [*Barnston et al.*, 1997] in July–September (JAS) for one or more of the clusters. Figure 3 shows the value of the highest correlation in each cluster for the NTC and ACE with Nino3.4 for the periods 1950–2006 and 1970–2006. One notices that the largest increase in the correlation value, other than that for 1 to 2 clusters (representing the choice of making any clusters), occurs from 2 to 3 clusters. The correlation values then remain level or slightly diminish until a very high number of cluster is present ($n = 10$). The NTC in the cluster with the highest correlation with Nino3.4 SST is shown in Figure 3b for all years and in El Niño and La Niña years. The NTC decreases considerably for a cluster number higher than $n = 3$,
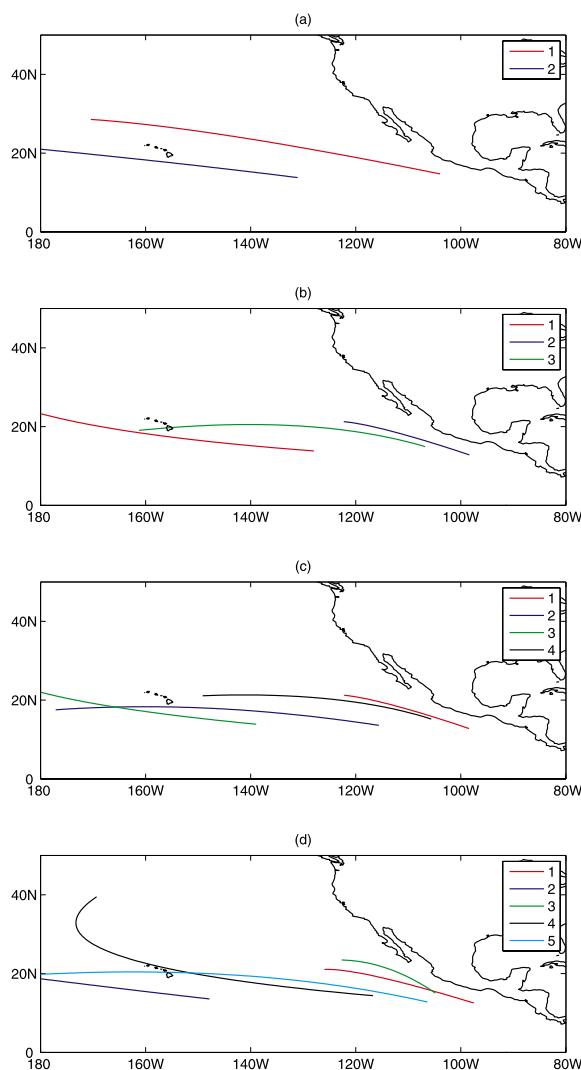

Figure 2. Regression trajectories of the TCs over the ENP, with (a) two, (b) three, (c) four, and (d) five clusters.

Therefore, this points to a choice of fewer clusters, i.e., $n = 3$ or $n = 4$.

[31] The final selection of the number of clusters n between $n = 3$ and $n = 4$ in this paper is then made on the basis of the relationship between the clusters and ENSO, as one of the main objectives of this paper is to examine the relationship between track types and ENSO. We would like to have an optimal number of clusters (3 or 4) chosen so as to obtain a significant value for the correlations of the number
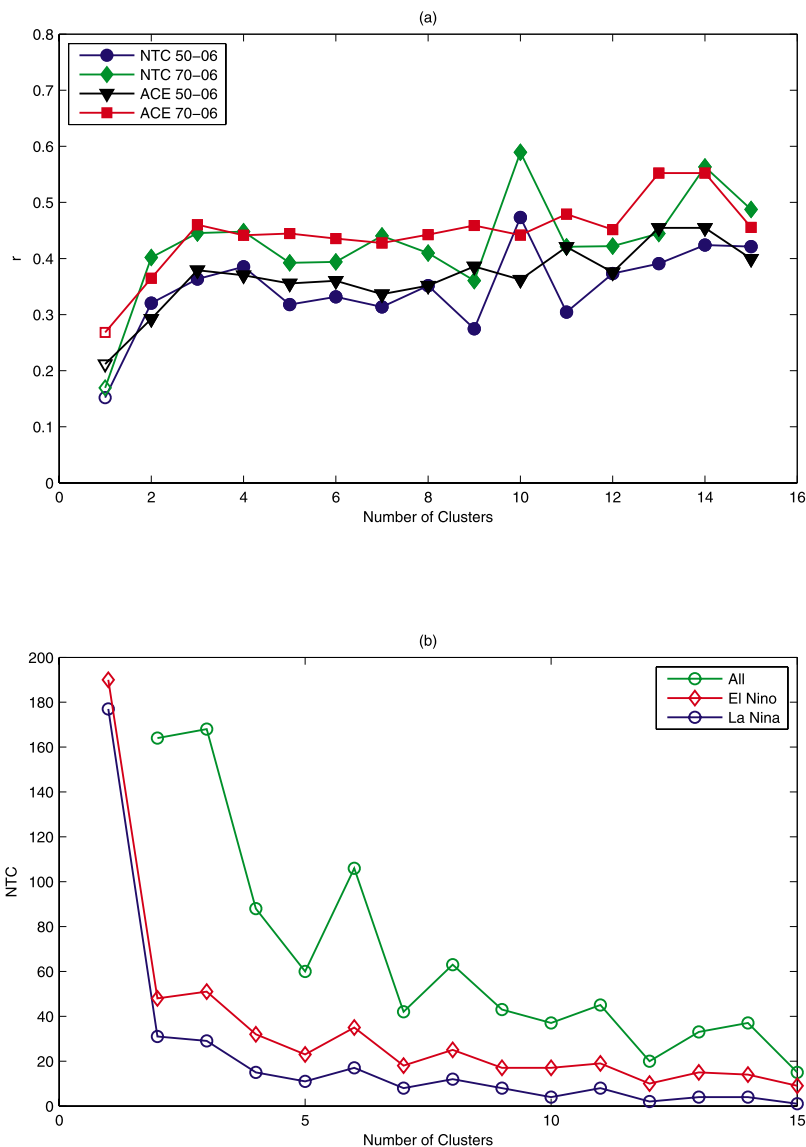
Figure 3. (a) Maximum correlation among the clusters for each total cluster value, between NTC and ACE and Niño3.4 JAS (July–September) in the periods of 1950–2006 and 1970–2006. Significant correlations are shown in solid symbols. (b) NTC in the cluster corresponding to the correlation in Figure 3a, for all years and El Niño and La Niña years.

especially in La Niña years; therefore the statistical significance of such cluster in La Niña years would be compromised if a higher number of clusters was chosen. Therefore, taking into account all these arguments, $n = 3$ seems to be the optimal choice in the trade-off balance between log-likelihood and error improvements, new information brought by adding a new cluster, the correlation value, and the size of NTC in each cluster for all ENSO phases.

[32] As discussed by *Kerr and Churchill* [2001], it is important to determine the stability of cluster analysis, using a bootstrapping method, for in-

stance. In order to examine the stability of our three-cluster solution, we examine the distribution of polynomial coefficients resulting from 100 integrations of the clustering algorithm using 50% subsamples of the tracks, drawn at random without replacement. For each cluster, Figure 4 shows the 3 polynomial regression coefficients for longitude (A_O, A_1 and A_2) together with those for latitude (B_O, B_1 and B_2), with the subscripts corresponding to the polynomial order [see *Gaffney et al.*, 2007, equation (2)]. The coefficients of the original reference run is always within the interquartile range of the distribution, in many cases very near
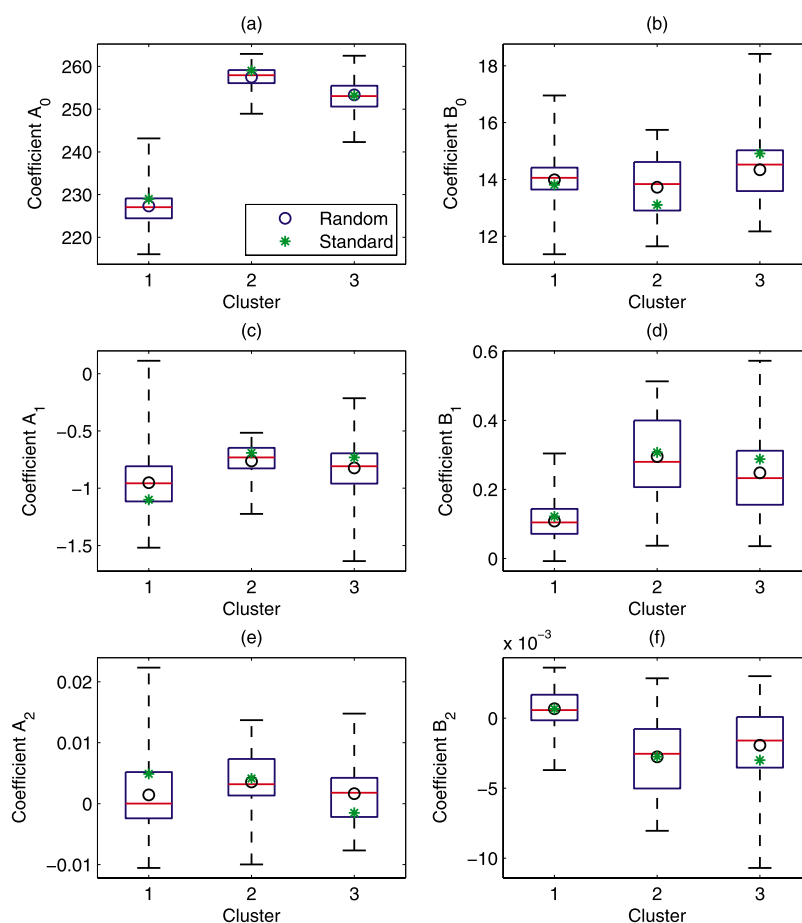
Figure 4. Polynomial coefficients distributions for 100 integrations of the cluster model using as input 50% subsamples of the tracks, drawn at random without replacement. The boxes show the 25th and 75th percentiles, the red lines in the boxes mark the median, the blue circles mark the mean, and the whiskers mark the values below (above) the 25th (75th) percentiles of the distribution. The green asterisks show the three-cluster solution coefficients. Polynomial coefficients for the (left) longitude and (right) latitude. The A and B coefficients subscripts correspond to the polynomial order.

the mean (blue circle) or median (red line) of the distribution.

[33] We also analyzed (not shown) the coefficients obtained when only ENSO neutral years are used. The main difference in the coefficients for neutral year occurs in cluster 1. As will be further discussed in the paper, cluster 1 is the most associated with the ENSO condition. In most cases, the coefficients for neutral years are within the range of the random integration coefficients.

[34] In order to access possible trends of the best track data set, presatellite and postsatellite, we also applied the cluster to tracks in the postsatellite era only (1970 and later). The coefficients of the postsatellite data (not shown) are not markedly different from those using the full best track data set.

3.2. Definition of ENSO Years

[35] The monthly SST index for the Niño3.4 area (5°S–5°N; 170–120°W) [*Barnston et al.*, 1997] was used to define the phase of ENSO, obtained from the Climate Prediction Center (CPC) for the period 1950–2006. We define El Niño (EN) and La Niña (LN) years according to the value of the Niño3.4 index averaged over the months of July to September (JAS), spanning the peak of the hurricane season in the eastern North Pacific. The 14 years (approximately 25% of the 57-year period) with the largest and smallest values of Niño3.4 in the period 1950–2006 are defined as EN and LN years, respectively; the remaining 29 years are classified as neutral years. The EN and LN years defined using our percentile method correspond to the Northern Hemisphere summers before the peaks of the ENSO events, and correspond well
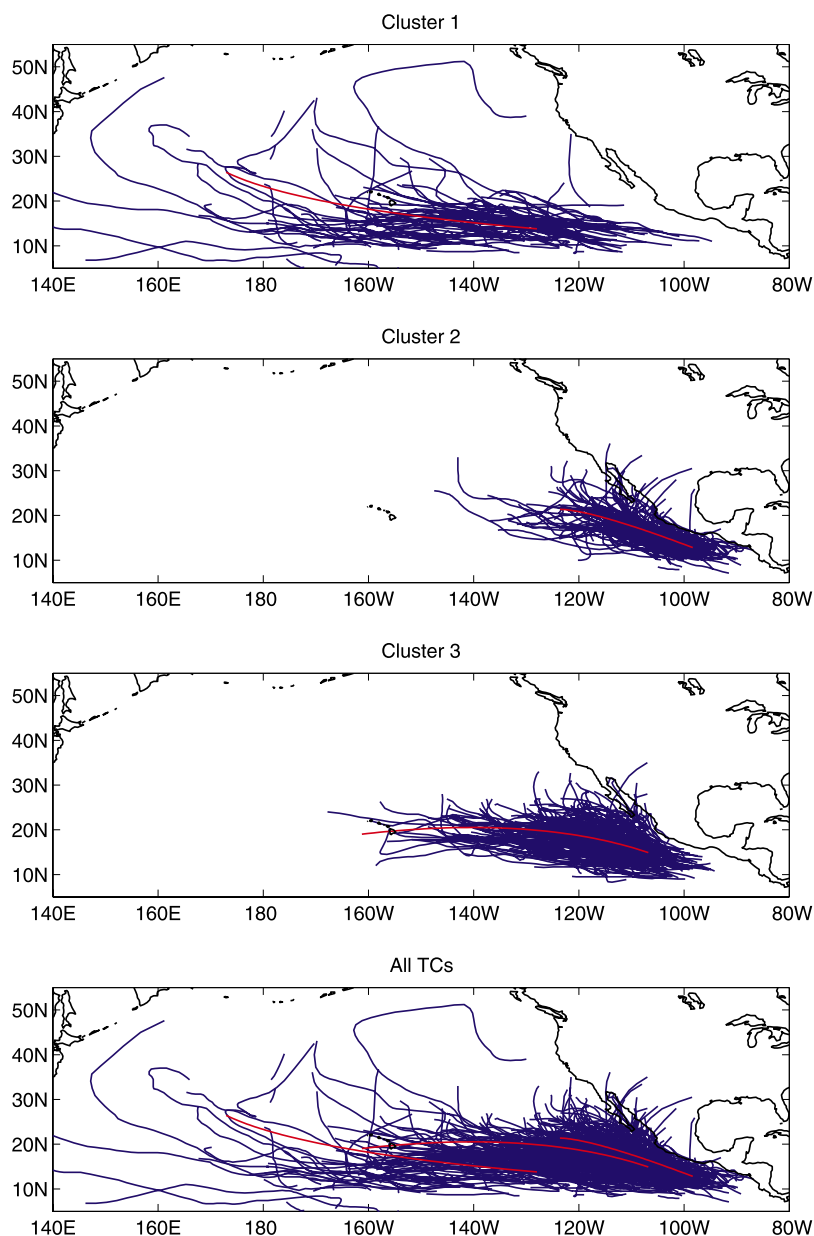
Figure 5. Eastern North Pacific TC tracks for three cluster types (in blue) and all TCs in the period 1980–2006. The regression trajectories of all TCs in each cluster (1949–2006) are shown in red. The regression model noise variances for the three models are (287.2, 26.6), (33.2, 10.1), and (26.3, 12.6), respectively (in degrees^2) where each pair denotes the longitude and latitude value.

to the ENSO events obtained using more traditional definitions. The same definition of ENSO events was used in various other studies [*Goddard and Dilley*, 2005; *Camargo et al.*, 2007b, 2007d].

4. Eastern North Pacific Hurricane Tracks Cluster Analysis

[36] We selected 3 clusters to best represent the ENP hurricane tracks with respect to ENSO, as described in section 3. The cluster analysis was based on all TC tracks with tropical storm intensity or higher in the best track data set for the period 1949–2006. The TC tracks within the period 1980–2006 are shown in Figure 5, together the mean trajectory for each cluster. The regression model noise variances are given in the caption.

[37] The number of TCs (NTC) in each cluster for the period 1950–2006 (when Niño3.4 data are available) is shown in Table 1. Approximately half

Table 1. Number of Tropical Cyclones (NTC), Number of Landfalls (NLF), and Percentage of Landfalls (PLF) for the ENP in El Niño, La Niña, Neutral, and All Years for Each Cluster and the Whole Basin

Cluster	La Niña			Neutral			El Niño			All Years		
	NTC	NLF	PLF	NTC	NLF	PLF	NTC	NLF	PLF	NTC	NLF	PLF
1	29	0	0%	88	1	1%	51	0	0%	168	1	1%
2	51	19	37%	121	42	35%	55	19	34%	227	80	35%
3	97	7	7%	231	24	10%	84	10	12%	418	41	10%
All	177	26	15%	440	67	15%	140	29	21%	813	122	15%

(418/813, or 51%) of the TCs belong to cluster 3, with a typical westward track. Cluster 2 TCs correspond to 28% of the total and have typical northwest tracks tending to follow the Mexican coastline. Only 21% belong to cluster 1, with tracks spreading farther west across the Pacific, with some TCs reaching the Central North Pacific.

[38] The cumulative density (number of TCs per 2° latitude/longitude square) of the first position of all TCs in each cluster is shown in Figure 6. The genesis locations of clusters 2 and 3 are very near the Mexican coast, with the cluster 2 maximum slightly to the northwest of the cluster 3 maximum. Cluster 1 genesis locations have a large spread compared with the other clusters and are located
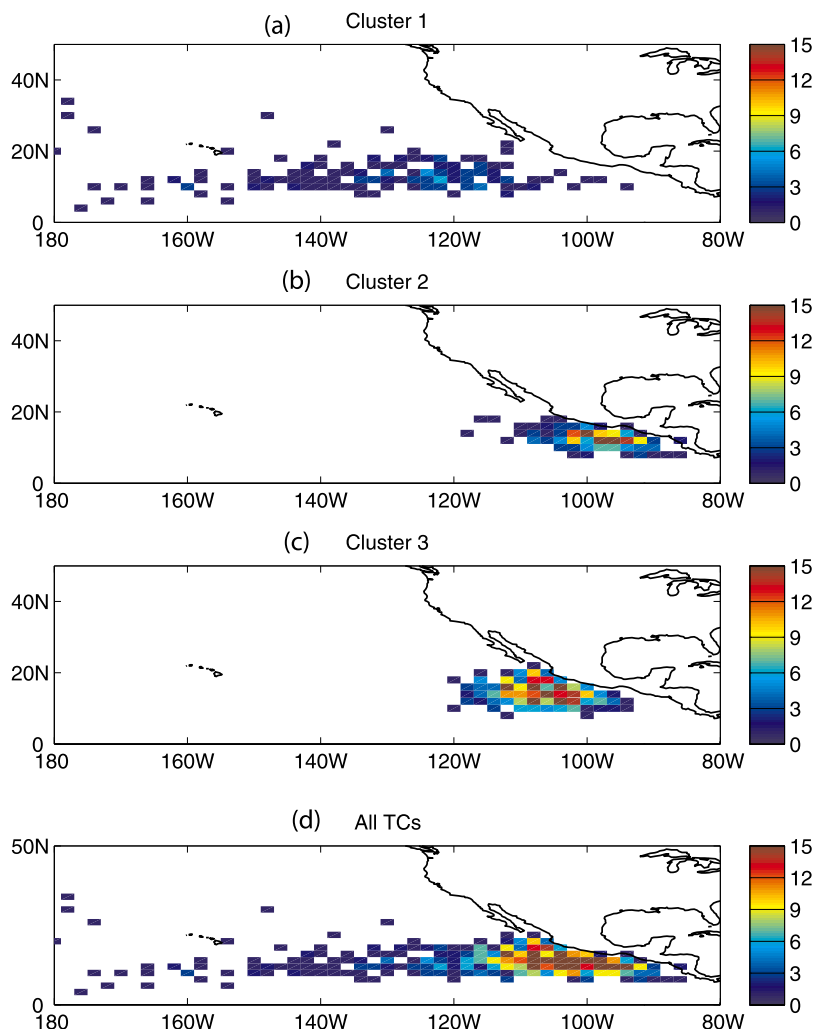

Figure 6. Cumulative density first position (total number of NTC in each 2° longitude and latitude) in the eastern North Pacific TCs in the period 1949–2006 (a–c) for the three clusters and (d) for all TCs.

Table 2. Average and Standard Deviation of TC First Position (Latitude and Longitude) for All TCs and All Years and Stratified by Either or Both of TC Cluster (Rows) and ENSO Phase (Columns)

	All Years	La Niña	Neutral	El Niño
Latitude				
All TCs	13.7°N ± 3.0	14.3°N ± 3.1	13.6°N ± 2.9	13.1°N ± 2.8
Cluster 1	13.4°N ± 4.1	15.5°N ± 4.9	13.4°N ± 4.1	12.1°N ± 3.2
Cluster 2	12.5°N ± 1.9	12.6°N ± 1.8	12.6°N ± 2.1	12.3°N ± 1.7
Cluster 3	14.4°N ± 2.7	14.8°N ± 2.6	14.3°N ± 2.6	14.1°N ± 2.7
Longitude				
All TCs	250.7°E ± 14.6	252.3°E ± 14.0	251.2°E ± 13.3	248.0°E ± 17.7
Cluster 1	229.4°E ± 17.7	229.0°E ± 17.5	231.6°E ± 15.9	225.9°E ± 20.2
Cluster 2	261.6°E ± 5.1	263.6°E ± 4.7	261.2°E ± 5.1	260.8°E ± 5.1
Cluster 3	253.3°E ± 4.9	253.3°E ± 5.1	253.4°E ± 4.9	252.9°E ± 4.7

farther west. Note that some of the first positions in cluster 1 occur in the Central North Pacific region (west of 140°W to the dateline).

[39] The mean and standard deviation of TC first position for each cluster and for the full basin are given in Table 2. Besides the marked difference in longitudinal positions for each cluster, latitudinal differences also occur. The mean first position

latitude of cluster 3 (2) is located to the North (South) of the other 2 clusters.

[40] The mean NTC per month for each cluster and for all TCs is given in Figure 7. While the seasonal cycle of cluster 1 has a distinctive maximum in August, clusters 2 and 3 have much flatter distributions. Cluster 3 TCs occur mainly from June to October, with a peak number in July to September
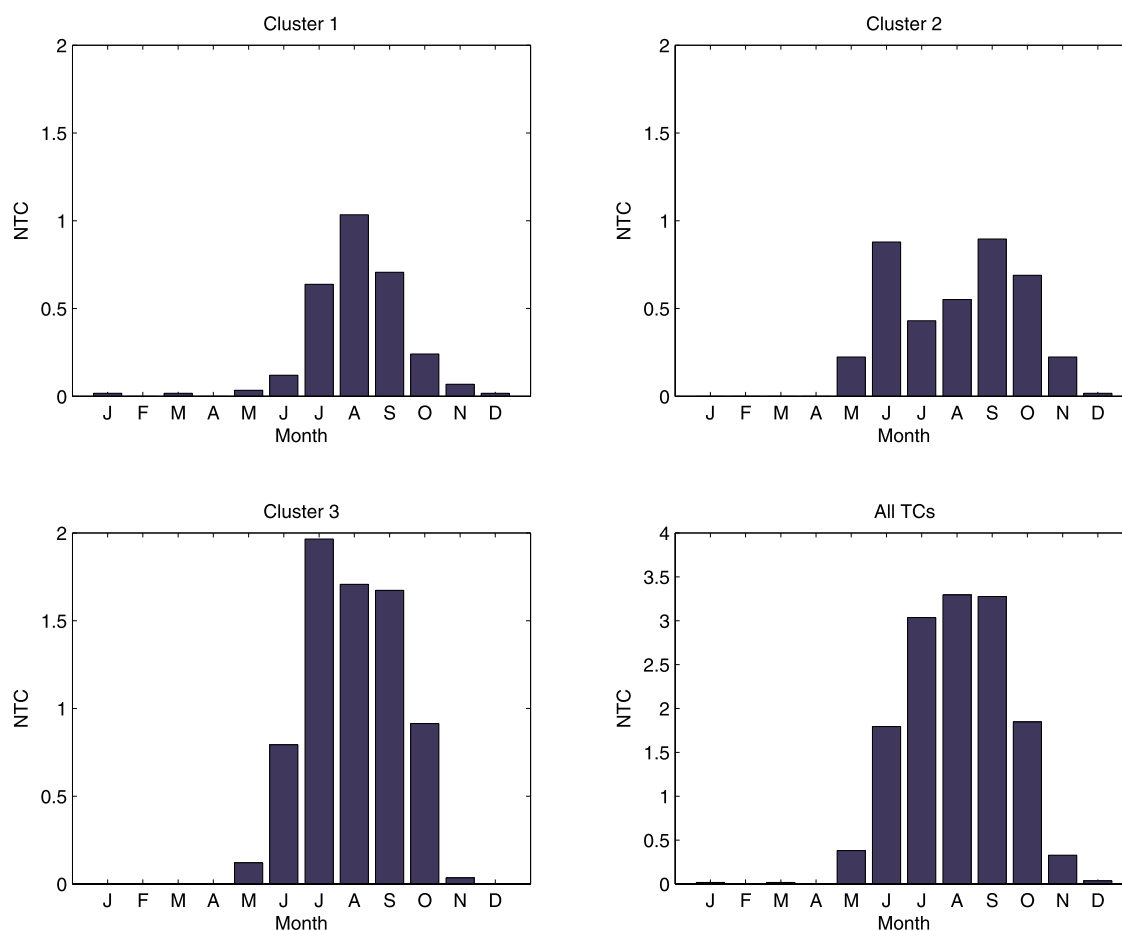

Figure 7. Eastern North Pacific mean NTC per month in the period 1949–2006 for the three clusters and all TCs.
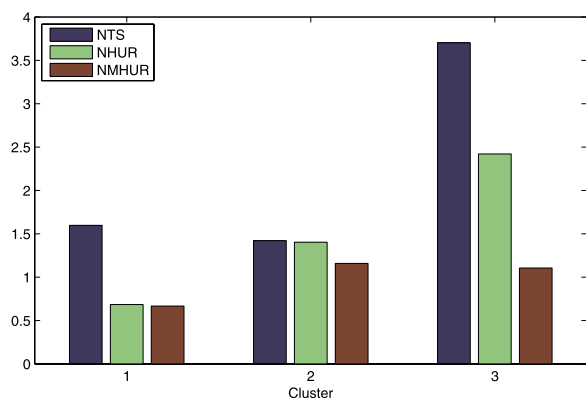
Figure 8. Eastern North Pacific mean NTC per category in the period 1949–2006 for the three clusters: NTS, number of tropical storms; NHUR, number of hurricanes of categories 1 and 2; NMHUR, number of major hurricanes with categories 3–5.

as found for all TCs collectively. In contrast, cluster 2 has a rather flat bimodal distribution with one maximum in June and another in September.

[41] The mean number of TCs in three intensity ranges (tropical storm, hurricane (categories 1–2), and major hurricane (categories 3–5)) for each cluster is shown in Figure 8. Cluster 2 TCs are almost equally divided into tropical storms, hurricanes and intense hurricanes, while in clusters 1 and 3, most TCs are tropical storms. Cluster 1 has a similar number of hurricanes and major hurricanes. The most frequent cluster type (3) has significantly more hurricanes than major hurricanes.

[42] The distribution of ACE (Accumulated Cyclone Energy) [*Bell et al.*, 2000] per TC in each cluster (not shown) reflects the distribution of the TCs per category. Cluster 2 has the distribution with the highest values of ACE per storm, because of the relatively higher number of major hurricanes in that cluster, compared with the other two. The distribution of ACE per storm reaching the lowest ACE values occurs in cluster 3, which has relatively fewer major hurricanes than the other clusters.

[43] The number and percentages of landfalls per cluster are also given in Table 1. The cluster with the highest percentage of landfalls is cluster 2 (35%), the tracks in cluster 2 tending to parallel the Mexican coast, with some of them recurving and making landfall in Mexico. The most populated cluster (cluster 3) has considerably fewer landfalls than cluster 2, as cluster 3 tracks are directed westward compared to cluster 2. Only one TC belonging to cluster 1 made landfall in Hawaii (tropical storm # 7, in August 1958). However,

note that here we only consider cases in which the center of the TC is over land; the percentages would increase considerably if we also include TCs that do not make landfall, but are close enough to bring rainfall and wind impacts over land.

[44] The lifetime distribution for all TCs and by cluster is shown in Figure 9. TCs in cluster 3 tend to have the shortest lifetime with a mean value of 5.8 days, while clusters 1 and 2 have longer life spans, with means of 6.8 and 6.7 days, respectively. Cluster 1 has the distribution with a the largest spread, including some TCs with very long lifetimes: The 90 percentile for lifetimes are 15.4, 11.0, and 9.9 days for clusters 1–3, respectively. The longevity of TCs in cluster 1, coupled with their long, westward reaching tracks, can bring impacts to Hawaii and even into the central and western North Pacific regions. One of the reasons that the lifetimes in cluster 3 can be so large is that the TCs in that cluster almost never make landfall, landfall being one of the major contributors to early demise of TCs.

5. Relationship of ENP Hurricane Tracks With ENSO and MJO

[45] We now analyze how each cluster is related to ENSO. The number of TCs is much higher in El
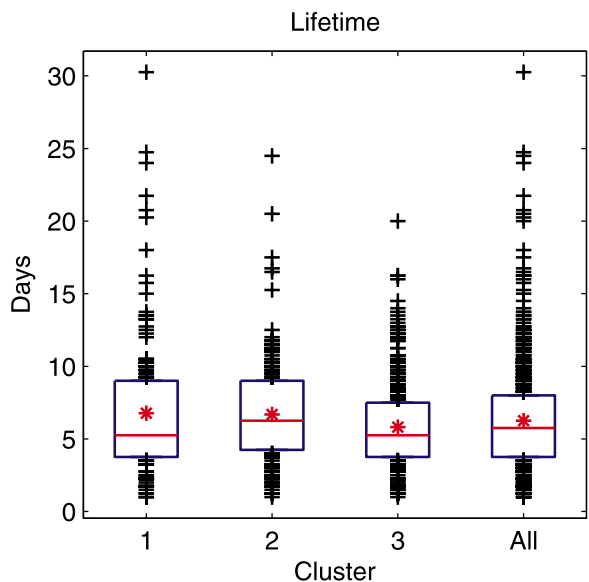

Figure 9. Distribution of lifetime per cyclone, in each cluster and for all TCs in the period 1949–2006. The boxes show the 25th and 75th percentiles, the red lines in the boxes mark the median, the asterisks mark the mean, and the crosses mark the values below (above) the 25th (75th) percentiles of the distributions.
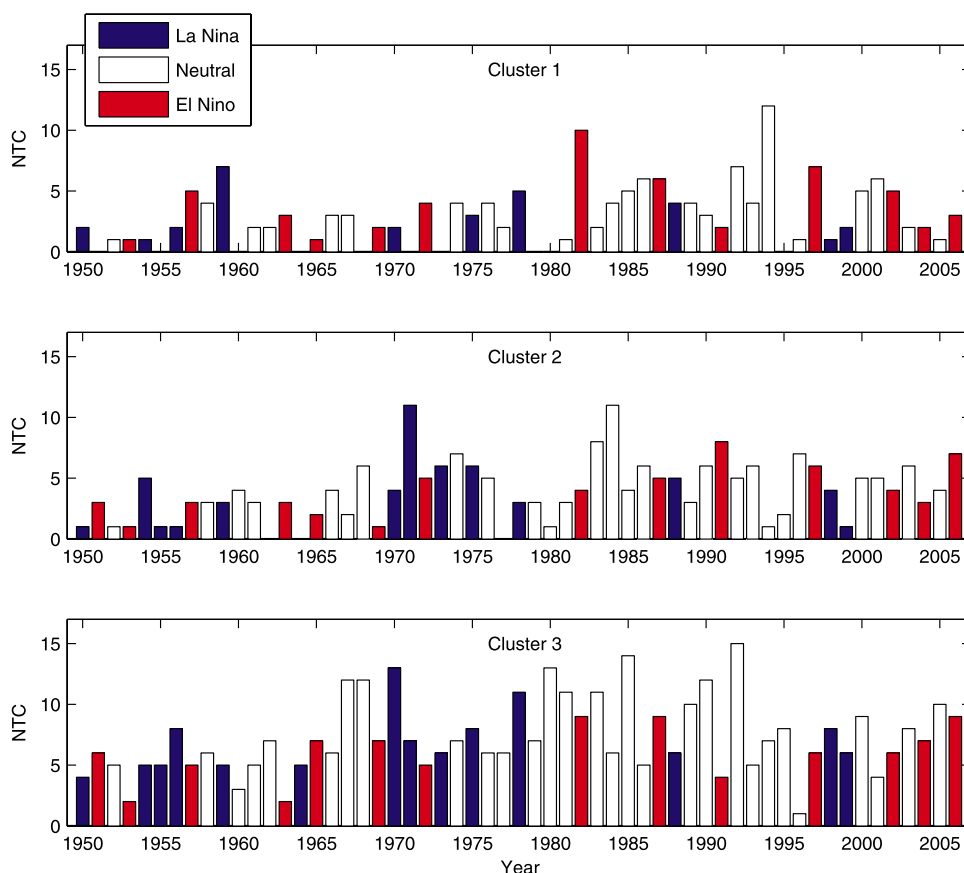
Figure 10. Number of cyclones (NTC) per year in each cluster in the period 1950–2006. EN (LN) years are shown in red (blue), and neutral years are shown in green.

Niño years (51 TCs) than in La Niña years (29 TCs) in cluster 1 (see Table 1), while the 2 other clusters have a similar number of TCs in El Niño and La Niña years.

[46] In Figure 10, we show the number of tropical cyclones per year in each cluster, with the ENSO phase denoted by the colors. The change points (1982, 1999) for high versus low-activity epochs that *Zhao and Chu* [2006] obtained for the whole ENP basin do not appear straightforwardly in the different clusters.

[47] As cluster 3 is the most populated cluster overall, in more than half of the years (39 out of 57) it contains more TCs than either of the other two clusters, and in 5 additional years it is tied with another cluster for this status. When the largest cluster is in its own above-normal tercile, the whole basin tends to be in the above normal tercile to a greater degree than when either of the other two clusters are in their own above-normal terciles.

[48] The higher NTC values in El Niño years, such as 1982, 1987, 1997 in cluster 1 are noticeable, while the 2 other clusters do not show systematic NTC shifts in response to the ENSO phase. The correlation of NTC, or ACE, per year for each cluster and for all TCs with Niño3.4 in JAS, is given in Table 3. Only cluster 1 has significant positive correlations between TC activity and

Table 3. Correlations Between the Number of Tropical Cyclones (NTC) and Accumulated Cyclone Energy (ACE) per Year in the Eastern North Pacific With Niño3.4 JAS (July–September) for Each Cluster and for All TCs in the Periods 1950–2006 and 1970–2006[a]

Cluster	NTC		ACE	
	50–06	70–06	50–06	70–06
1	**0.36**	**0.44**	**0.38**	**0.46**
2	0.06	0.00	0.02	0.00
3	−0.10	−0.16	0.01	−0.03
All	0.15	0.17	0.21	0.27

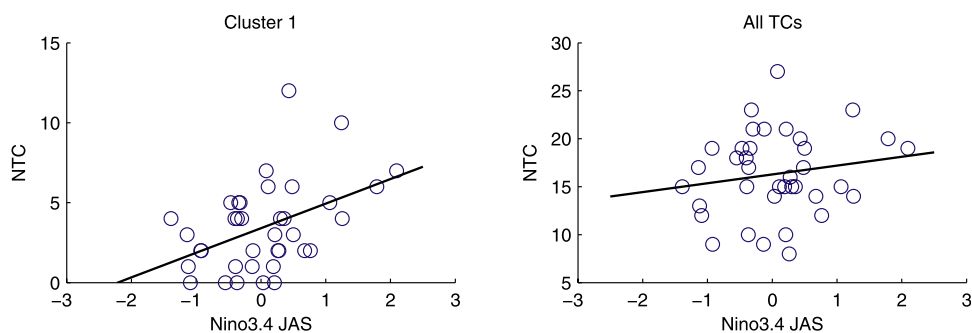[a] Significant correlations at the 95% level are in bold.

Figure 11. Scatterplot of NTC and Nino3.4 JAS for cluster 1 and for all TCs in the period 1970–2006 (blue). The regression lines are shown in black.

Niño3.4. Therefore, the main impact of El Niño in the eastern North Pacific is the more frequent occurrence of TCs with the type of tracks described by cluster 1, while the opposite occurs in La Niña years.

[49] Scatterplots of NTC and Nino3.4 JAS for cluster 1 and for all TCs for the period 1970–2006 are shown in Figure 11. The increase of NTC with Nino3.4 in cluster 1 is clear, with a weak tendency toward higher NTC with Nino3.4 sug-
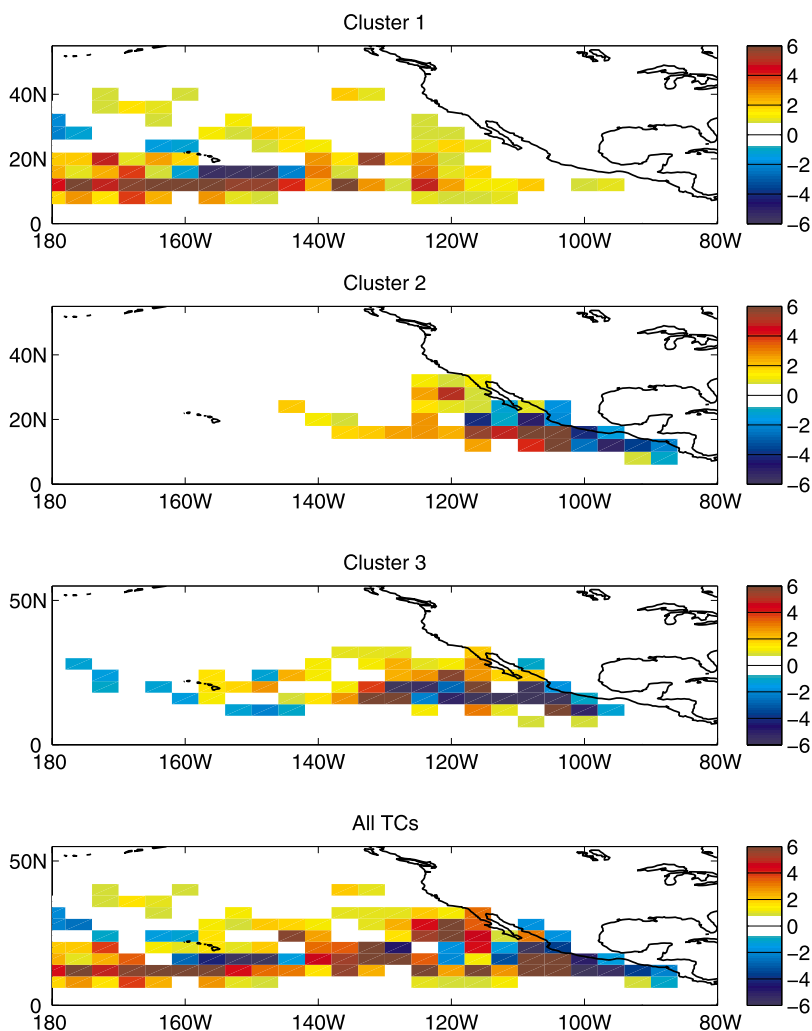

Figure 12. Track density difference between El Niño and La Niña years for each cluster and all TCs. The resolution is $4° \times 4°$.
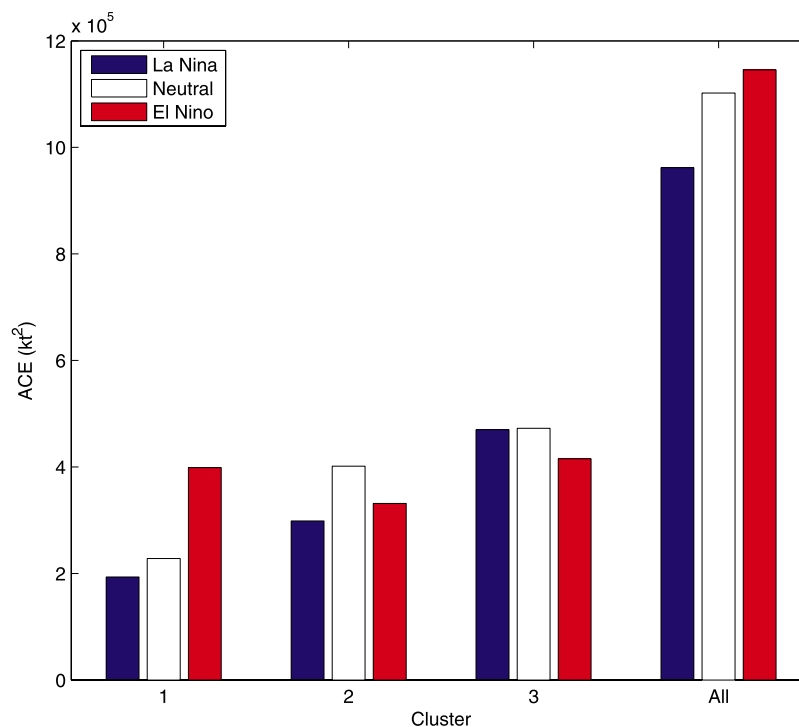
Figure 13. Mean accumulated cyclone energy (ACE) per year in $(kt)^2$, per cluster and for all TCs, in La Niña, neutral, and El Niño years.

gested for all TCs. Scatterplots for ACE (not shown) are very similar. The similarity between the correlation values for NTC and ACE suggests that the intensity of the TCs and the length of the tracks are not significantly altered by ENSO (not shown), although the ACE may mask opposite changes between the two variables. Clusters 2 and 3 are not significantly impacted by the ENSO state.

[50] The NTC distribution is shifted toward higher values in El Niño years for cluster 1, compared to La Niña and neutral years. The 25th and 75th percentiles of the NTC distribution for cluster 1 are 0, 1, 2 and 3, 4, 5, respectively, for La Niña or neutral years, versus El Niño years. Such a shift does not occur for the other 2 clusters. However, the dominant cluster most years, including El Niño years, is still cluster 3, as discussed above.

[51] To examine in more detail the difference of TC activity in El Niño and La Niña years, we calculated the cumulative track density (number of track days in each 2° longitude and latitude square) difference of El Niño and La Niña years (Figure 12). When all TCs are considered, there is a decrease in TC activity near the Mexican coast and a increase in activity in the western part of

the basin in El Niño years (Figure 12). By comparing with the difference of EN and LN track density in each cluster, we can identify the increase in western part of the basin being associated mainly with cluster 1, while the decrease near the coast and a northward shift (mainly between 105° and 125°W longitude) are the most significant changes in Cluster 3. Therefore, there is a shift westward of the TC activity in the basin in El Niño years compared with La Niña years, due to more westward tracks of the type characterized in cluster 1 [*Kimberlain*, 1999; *Wu and Chu*, 2007].

[52] Table 2 stratifies the mean first position by ENSO phase, for the whole basin and for each cluster. The westward shift in first position in El Niño years occurs for the full basin and also in all 3 clusters (not only in cluster 1). There is also a noticeable latitudinal shift toward the equator in El Niño years, and higher latitudes in La Niña years. This latitudinal shift is similar to what occurs in the Western North Pacific, while the longitudinal shift is in the opposite sense [*Chia and Ropelewski*, 2002].

[53] The mean ACE in each ENSO phase per cluster and for all years is shown in Figure 13.
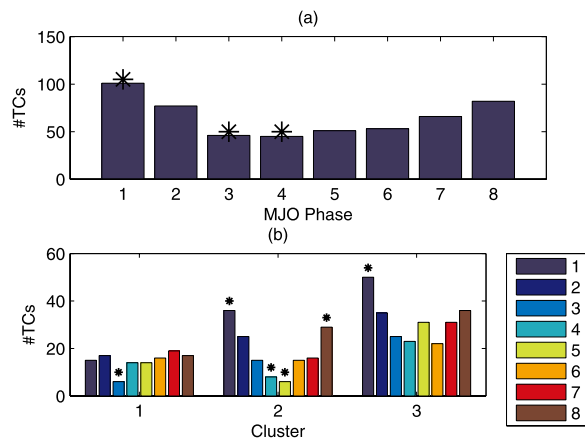
Figure 14. (a) NTC per MJO phase and (b) NTC in each cluster per MJO phase. Asterisks indicate statistical significance at the 99% level.

The mean ACE value for cluster 1 is higher in EN compared to LN and neutral years, and this is reflected in the overall basin. The mean ACE value for cluster 2 is very similar for EN and LN years, while for cluster 3 the mean ACE value is slighter smaller in EN years compared to LN and neutral years. ACE values include number, intensity and life span of the TCs, so higher ACE values are due to a combination of these 3 factors, with more weight on the intensity of the TCs, as the wind speed is squared in the ACE definition.

[54] It is well known that the MJO [*Madden and Julian*, 1972] modulates tropical cyclogenesis in the ENP [*Molinari et al.*, 1997; *Maloney and Hartmann*, 2000, 2001; *Hartmann and Maloney*, 2001]. When the MJO phase is westerly over the region (based on 850 hPa zonal winds), the conditions are more propitious for cyclogenesis, and the enhanced cyclogenesis that occurs is often clustered in time.

[55] We stratified the genesis of the TCs according to the eight phases of the MJO, as defined by *Wheeler and Hendon* [2004], for all TCs and for each cluster (see Figure 14). The Wheeler and Kiladis index is available starting only in 1974, so only TCs that occur after 1974 were included in this analysis. The statistical significance in Figure 14 was calculated using a bootstrap method, in which random MJO phases were assigned to TCs a large number of times (1000). The random assignment keeps the number of TCs in each cluster fixed, only randomizing the MJO assignments for the number of TCs in each cluster. If the number of TCs in a specific cluster and MJO phase

is larger (smaller) than the 99% (1%) percentile of the random uniform distribution for that cluster, the number of TCs in that cluster and MJO phase is considered statistically significant.

[56] When all TCs are considered, there is a statistically significant enhancement of cyclogenesis in the ENP (99% significance level), when the MJO is in phase 1 (Western Hemisphere and Africa). In phases 3 and 4 (Indian Ocean and Maritime continent) of the MJO there is a statistically significant suppression of the cyclogenesis in the ENP. *Wheeler and Hendon* [2004, Figure 9] show that in phase 1 of the MJO in May-June, there is anomalous convection (as given by outgoing long-wave radiation (OLR)) east of the dateline and anomalous westerlies in the ENP region. In contrast [see *Wheeler and Hendon*, 2004, Figure 9], in phases 3 and 4, the center of anomalous convection is over the Indian Ocean and Indonesia and there are anomalous easterlies in the ENP. These results are in agreement with the work of *Molinari et al.* [1997] and *Maloney and Hartmann* [2000], who noticed the enhancement (suppression) of cyclogenesis in the ENP when the anomalous low-level winds in the region are westerly (easterly), which determined their definition of the MJO.

[57] As expected, cyclogenesis in cluster 3 (the most populated cluster) is enhanced when the MJO is in phase 1, reflecting what happens for all TCs. The number of TCs in cluster 2 for phases 1 and 8 is also enhanced, with the suppression in phases 4 and 5 (MJO at Maritime Continent) also being statistically significant. Cluster 2, therefore, is strongly modulated by the MJO, both in enhancement and suppression. This result takes on particular importance considering that cluster 2 has the highest landfall rate in the western Mexican coast. Landfall occurrences in that cluster appear to be influenced by the MJO phase. Interestingly, cluster 1, which is strongly related to ENSO, is not substantially impacted by the MJO. Only in phase 3 of the MJO there is a significant suppression of TCs in cluster 1.

[58] When the cluster technique is applied to tracks that occur in neutral ENSO years only and the number of TCs in each MJO phase is analyzed, the result obtained is very similar to the discussion above. There is a statistically significant enhancement (suppression) in the number of TCs when the MJO is in phase 1 (3), similar to Figure 14a. When the TCs for neutral years are first stratified by cluster and then in MJO phase, the only statistically

significant results are for cluster 1 (suppression of TCs in the phase 3) and for cluster 2 (enhancement in phase 1 and suppression in phase 6), again not very distinct from Figure 14b. It is important to note that not many TCs are included in this latter analysis in each cluster and MJO phase, as only neutral years are considered and the MJO index is only existent after 1974.

6. Environmental Composites

[59] We constructed composites of large-scale circulation patterns associated with each cluster by compositing the days that correspond to either the first position or 2 days prior to the cyclogenesis. The rationale for choosing the first position is the potential usage of these patterns in tracks and landfall forecasts, once the genesis position of a cyclone is known. Besides, the large-scale circulation patterns that control genesis and track type are not independent of one other, since they are associated with different positions and intensities of the monsoon trough and subtropical ridge. In some cases we make the composites 2 days prior to the genesis if no other TC is present; that way only the environmental flow is present in the composite, without any TCs. The number of TCs included in each composite varies by cluster, and also by the length of the available data set for the variable in question (OLR, SST, wind fields, etc). Here we show just a few of these composites.

[60] Our approach is the same as that used by *Camargo et al.* [2007a], which differs from the methodology used by *Vincent and Fink* [2001] and *Fink and Vincent* [2003]. These authors made composites for specific locations in the region using first a classification of the systems into weak, strong, intensifying and dissipating. One of the key points of their results is the contrasting characteristics between the western and ENP environments favorable for TCs, and the influence of dry air in TCs. A review of the climatological atmospheric conditions in the ENP is given *Amador et al.* [2006].

[61] Figure 15 shows the sea surface temperature (SST) anomaly composites for each cluster and for all TCs in the period 1982–2006. The anomalies for all TCs are weakly warm over the Pacific. Cluster 1 SST anomalies are very typical of El Niño anomalies. Cluster 3 weakly suggests a La Niña signal. In all clusters, anomalously warm SSTs are present in the cyclogenesis region near Gulf of Tehuantepec and Gulf of California. This is

the region with highest cyclogenesis frequency in the ENP, and locally higher SST is associated with greater cyclogenesis.

[62] In Figure 16 the anomalous OLR outgoing long-wave radiation (OLR) at first position, and the anomalous environmental winds 2 days before the first position, are shown. The wind composites were calculated prior to the existence of the TC so that the TC winds themselves would not be included in the composite. The OLR anomalies of cluster 1 is centered on 120°W, west of the two other clusters OLR anomalies. In clusters 2 and especially 3, negative anomalies are concentrated in a small region where most of the TCs occur. In cluster 2, the negative OLR anomalies extend into the Gulf of Mexico. The westerly anomalies in clusters 2 and 3 extend from the equator to approximately 10°N, while in the case of the cluster 1, they are restricted to the equatorial region, with anomalous easterlies occurring northward of 7.5°N.

[63] Although the wind composites were defined 2 days prior to the TC formation so that mainly environmental winds (not TC winds) would contribute, cyclonic wind anomalies are clearly present in cluster 3 at the location of TC formation. This suggests cyclonic motion as a precursor, or the possible presence of another earlier TC and that could include tropical depressions, which were not taken into account in this analysis. Easterly anomalies from the Atlantic to the eastern Pacific around 10–20°N are present in all composites, with the easterly anomalies reaching different longitudes, depending on the cluster, extending to 130°W in cluster 1.

[64] Composites of the anomalous vorticity at 850 hPa (not shown) have regions of anomalous cyclonic vorticity in the regions of main cyclogenesis in clusters 2 and 3. In cluster 1, the cyclonic vorticity region is larger, coinciding with the region of convection shown for that cluster in Figure 16. It is important to note that in cluster 1 there is an anticyclonic anomaly west of the Mexican coast, while in the other two clusters the anomaly there is cyclonic. This is consistent with the formation of cyclones in cluster 1 being farther to the west than in the other two clusters.

[65] Zonal 850 hPa wind anomaly composites are shown in Figure 17. Anomalous westerlies are present in the composites for all clusters near or south of 10°N. However, the longitude of these westerly anomalies differ widely by cluster. In
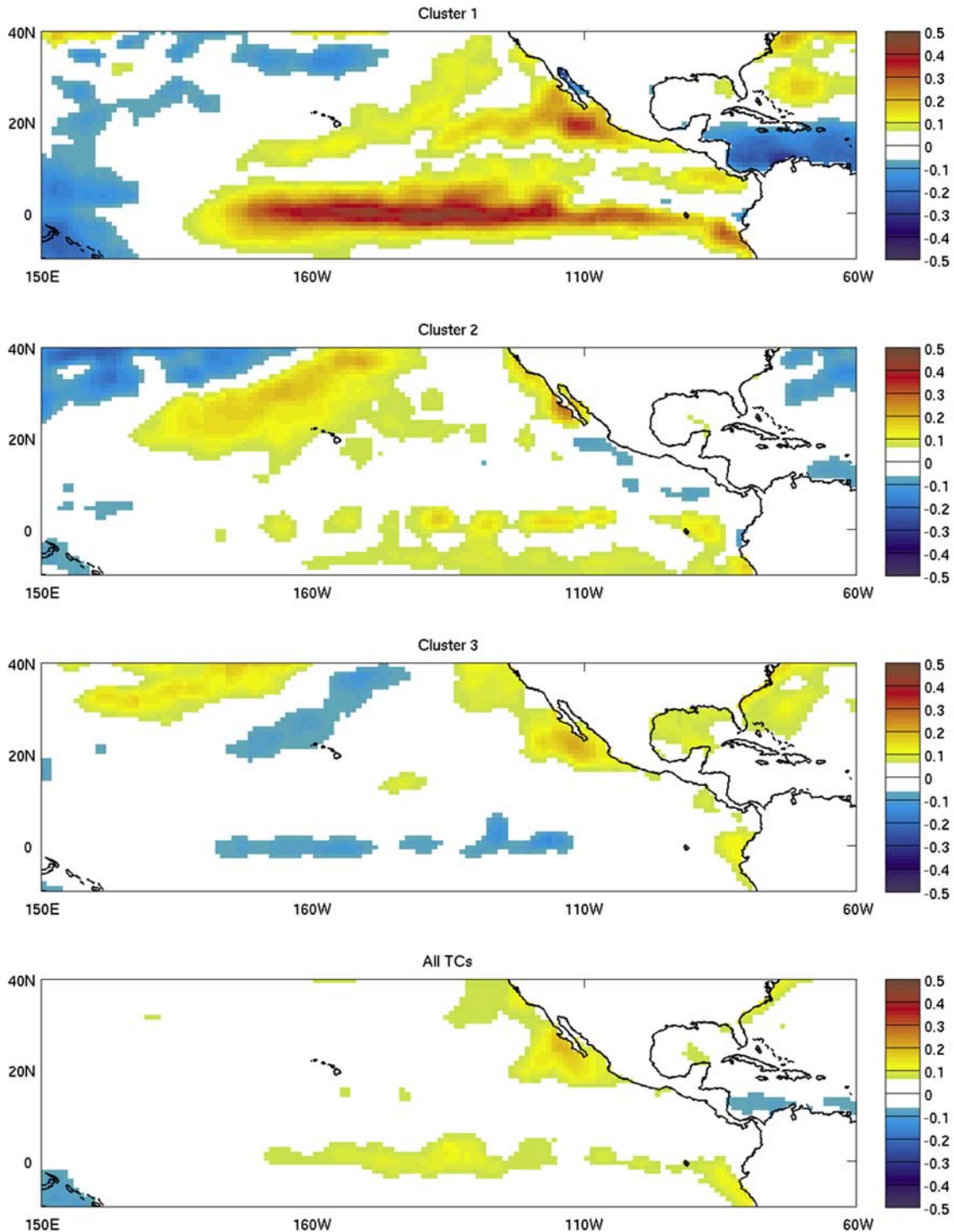
Figure 15. Composites of weekly sea surface temperature anomalies (°C) in each cluster and for all TCs in the period 1982–2006.

previous studies [e.g., *Molinari et al.*, 1997], it has been stated that cyclogenesis occurs preferentially in the region where the easterlies from the Atlantic meet the anomalous westerlies characteristic of the monsoon trough in the Pacific. The longitude at which this confluence occurs may be a key factor distinguishing the clusters defined here. For example, the shift to the west of the confluence region in
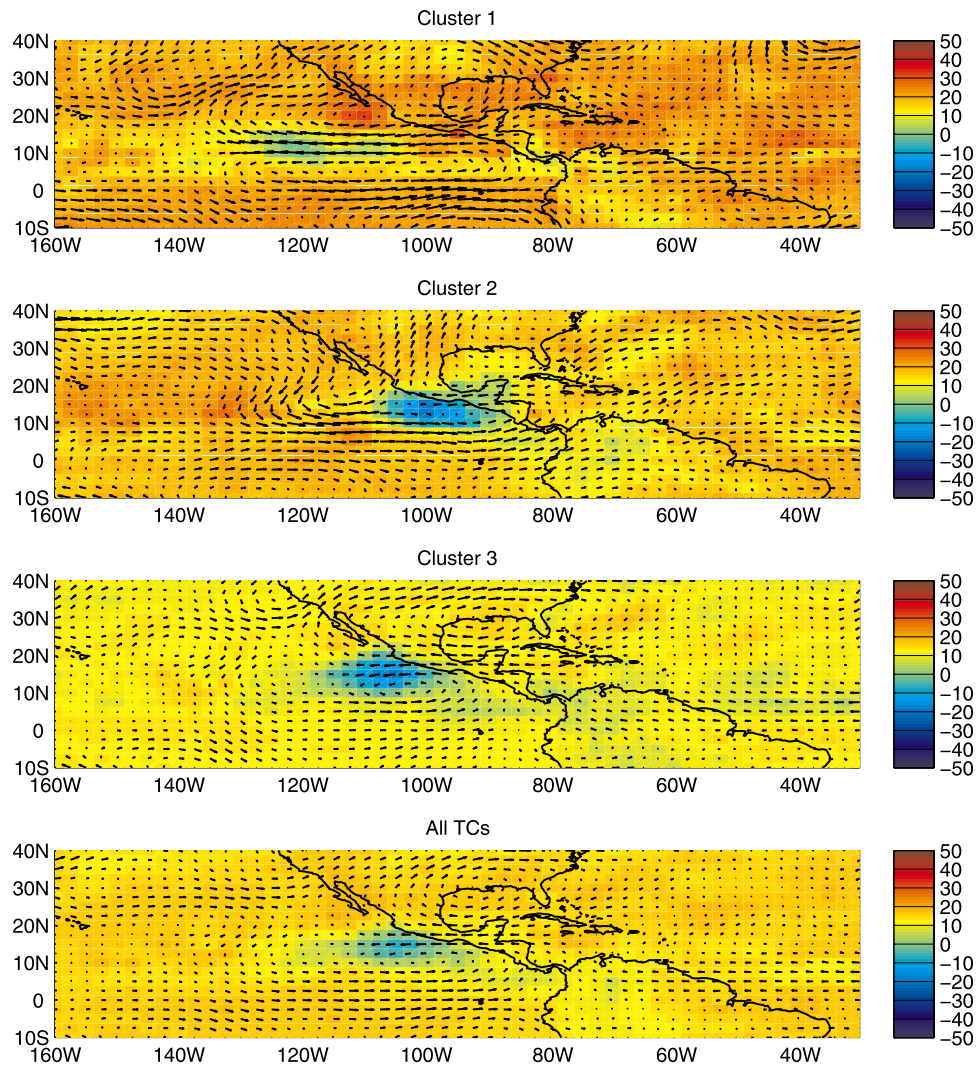
Figure 16. Composites of monthly OLR anomalies (W/m²)at genesis (color, 1974–2006) and monthly 500 hPa wind anomalies (2 days) prior to genesis (arrows, 1950–2006) for the three clusters and all TCs.

cluster 3 relative to cluster 2 leads to a westward shifted cyclogenesis location in cluster 3. The anomalous westerlies in cluster 1 are not as localized as in clusters 2 and 3, and are weaker. The anomalous easterlies in cluster 1 are stronger and pervasive over a larger area of the ENP. Relatively stronger westerlies occur in cluster 2, the cluster most strongly modulated by the MJO. As noted by *Maloney and Hartmann* [2000], cyclogenesis is enhanced in the ENP when the MJO is in its westerly phase, as determined by the zonal wind at 850 hPa. Therefore, these composites confirm the *Molinari et al.* [1997] and *Maloney and Hartmann* [2000] findings, and identify which type of tracks is mostly affected by the westerly anomalies described in their study.

[66] Environmental composites for the cluster analysis using neutral ENSO years only were also calculated. The composites for clusters 2 and 3 are very similar to the composites for all years, shown above. As could be expected, differences occur in cluster 1, as the El Niño characteristics of the composites are not present. For instance, in the zonal wind anomaly composites for cluster 1 for neutral years, the westerly anomalies are concentrated near the Asian continent, not extending throughout most of the basin as occurs when all years are considered (Figure 17).

[67] The environmental composites shown are in agreement with our analysis of the TCs in each cluster. When there is a westerly phase of the MJO occurring in the ENP, there is a higher probability of cluster 2 type tracks to occur, even if during
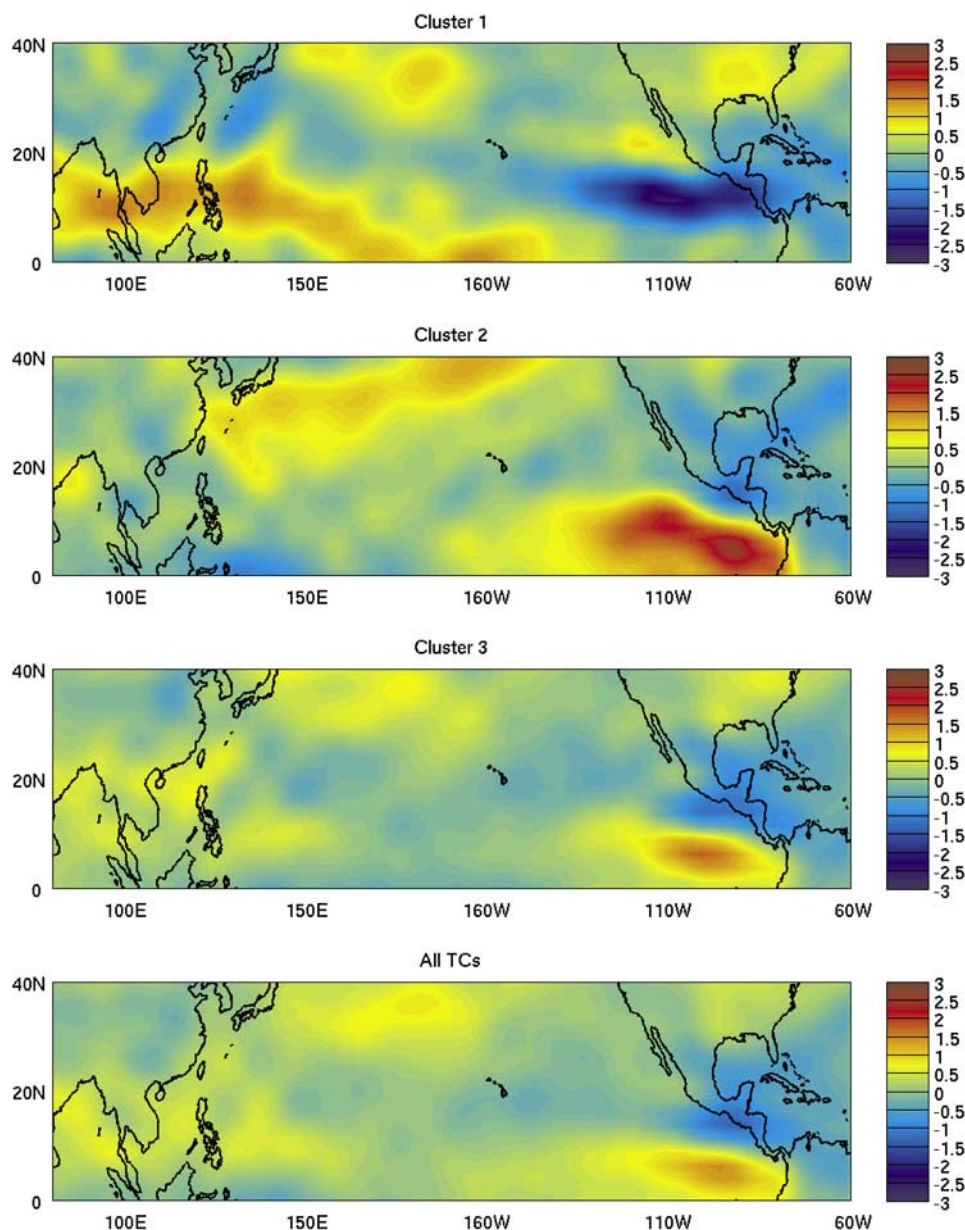
Figure 17. Composites of monthly zonal wind anomalies (m/s) at 850 hPa for the three clusters and all TCs in the period 1950–2006.

most of the season the cluster 3 track type is more frequent. During these MJO episodes, therefore, there is a higher chance of TCs making landfall in Mexico.

[68] In warm ENSO years, there is a higher probability of occurrence of TCs forming further from the coast and these could affect the Hawaii Islands. These track types will occur when the anomalous monsoon westerlies extension reaches the dateline and further. The occurrence of these westerly anomalies will depend on the onset timing of the

El Niño and the strength of the episode. During the ENP peak hurricane season (JAS), ENSO episodes are usually not yet at their peak, which usually occur in the northern hemisphere autumn and winter.

7. Summary

[69] In this paper, we applied a probabilistic clustering technique based on a regression mixture model to describe ENP TC tracks. Each component of the mixture model consists of a quadratic

regression curve of cyclone position against time together with a noise variance for each observed TC position given the model. A three cluster solution was chosen to best describe the locations and shapes of the tracks in this region and their relationships with ENSO and MJO.

[70] The smallest cluster of tracks, i.e., the one that occurs least frequently, is associated with ENSO events, with significantly more TCs happening in El Niño years. This cluster (1) is characterized by tracks that form in a more westward location than those of the two other clusters, and some TCs reach the central and western North Pacific, and can impact Hawaii. Cluster 1 composites of circulation and OLR have different properties compared to the other 2 clusters, with broad-scale easterly anomalies extending westward from the Caribbean, and equatorial westerly anomalies in the central equatorial Pacific. The OLR anomalies also occur over a broader region than in the other 2 clusters.

[71] Clusters 2 and 3 are much more similar to each other than to cluster 1. Both clusters have genesis locations just off the Mexican coast, very near the continent, with cluster 3 (the most frequent), displaced slightly to the southwest of cluster 2. Tracks in cluster 2 are typically nearer the coast and lead to a higher frequency of landfall. While both clusters are more prevalent in the westerly phase of the MJO (associated with enhanced convection in the region), cluster 2 is particularly strongly modulated by it, and is suppressed in the MJO's easterly phase. Cluster 3 is the most frequent trajectory type, with a west-northwest track and a low frequency of landfalls.

[72] The three-cluster solution provides a parsimonious description of ENP TCs that brings together the findings of the many previous studies; the ENSO relationship is described by cluster 1, while the MJO association is especially clear in cluster 2. Longitudinal track location clearly plays a strong discriminating role in the solution, while the average track orientation also becomes more zonal toward the west.

[73] Thus, while the conventional approach to investigating relationships with SOI and the MJO has been to stratify TC activity by the phase of the respective index (e.g., *Irwin and Davis* [1999] for SOI and *Maloney and Hartmann* [2000] for the MJO), the regression-based clustering reveals both relationships in terms of characteristics trajectory type.

[74] The relationship of specific track types with the MJO and ENSO phase could prove especially helpful for forecast guidance because track types that are associated with ENSO and MJO are expected to be have higher predictability than other track types. From a dynamical systems perspective, the system "states" are represented by the three TC clusters. These are populated in all years and through all phases of the MJO, but their prevalence is influenced by ENSO and the MJO. On the other hand, the magnitudes of these influences are relatively modest, underlining the necessity for a probabilistic model such as this in the forecasting context.

[75] In previous studies, the westward shift of the tracks with El Niño was noticed. But here we could specify that not all types of tracks are affected by ENSO, as the TCs that form near the coast, in clusters 2 and 3 are not modulated by ENSO. Therefore, impacts in Mexico will not be substantially modulated by ENSO, while they probably will be by an active MJO season. Our results are consistent with those reported in previous work on hurricane activity in this region, and further enhance the understanding of the modulation of TCs in the ENP by ENSO and MJO.

Acknowledgments

References

Amador, J. A., E. J. Alfaro, O. G. Lizano, and V. O. Magaña (2006), Atmospheric forcing of the eastern tropical Pacific: A review, *Prog. Oceanogr.*, *69*, 101–142.

Avila, L. A. (1991), Atlantic tropical systems of 1990, *Mon. Weather Rev.*, *119*, 2027–2033.

Avila, L., and R. J. Pasch (1992), Atlantic tropical systems of 1991, *Mon. Weather Rev.*, *120*, 2688–2696.

Barnston, A. G., M. Chelliah, and S. B. Goldenberg (1997), Documentation of a highly ENSO-related SST region in the equatorial Pacific, *Atmos. Ocean*, *35*, 367–383.

Bell, G. D., et al. (2000), Climate assessment for 1999, *Bull. Am. Meteorol. Soc.*, *81*, S1–S50.

Bister, M., and K. A. Emanuel (1997), The genesis of hurricane Guillermo: TEXMEX analyses and a modeling study, *Mon. Weather Rev.*, *125*, 2662–2682.

Bove, M. C., J. B. Elsner, C. W. Landsea, and X. Niu (1998), Effect of El Niño on U.S. landfalling hurricanes, revisited, *Bull. Am. Meteorol. Soc.*, *79*, 2477–2482.

Camargo, S. J., and A. H. Sobel (2005), Western North Pacific tropical cyclone intensity and ENSO, *J. Clim.*, *18*, 2996–3006.

Camargo, S. J., A. G. Barnston, P. J. Klotzbach, and C. W. Landsea (2007a), Seasonal tropical cyclone forecasts, *WMO Bull*, *56*, 297–309.

Camargo, S. J., K. A. Emanuel, and A. H. Sobel (2007b), Use of a genesis potential index to diagnose ENSO effects on tropical cyclone genesis, *J. Clim.*, *20*, 4819–4834.

Camargo, S. J., A. W. Robertson, S. J. Gaffney, P. Smyth, and M. Ghil (2007c), Cluster analysis of typhoon tracks. Part I: General properties, *J. Clim.*, *20*, 3635–3653.

Camargo, S. J., A. W. Robertson, S. J. Gaffney, P. Smyth, and M. Ghil (2007d), Cluster analysis of typhoon tracks. Part II: Large-scale circulation and ENSO, *J. Clim.*, *20*, 3654–3676.

Chan, J. C. L. (1995), Prediction of annual tropical cyclone activity over the western North Pacific and the South China Sea, *Int. J. Climatol.*, *15*, 1011–1019.

Chia, H. H., and C. F. Ropelewski (2002), The interannual variability in the genesis location of tropical cyclones in the northwest Pacific, *J. Clim.*, *15*, 2934–2944.

Chu, P. S. (2004), ENSO and tropical cyclone activity, in *Hurricanes and Typhoons: Past, Present and Future*, edited by R. J. Murnane and K.-B. Liu, pp. 297–332, Columbia Univ. Press, New York.

Chu, P. S., and X. Zhao (2007), A Bayesian regression approach for predicting seasonal tropical cyclone activity over the central North Pacific, *J. Clim.*, *20*, 4002–4013.

Collins, J. M., and I. M. Mason (2000), Local environmental conditions related to seasonal tropical cyclone activity in the northeast Pacific basin, *Geophys. Res. Lett.*, *27*, 3881–3884.

Elsner, J. B. (2003), Tracking hurricanes, *Bull. Am. Meteorol. Soc.*, *84*, 353–356.

Elsner, J. B., and A. B. Kara (1999), Hurricanes of the North Atlantic: Climate and Society, Oxford Univ. Press, New York.

Elsner, J. B., and K. B. Liu (2003), Examining the ENSO-typhoon hypothesis, *Clim. Res.*, *25*, 43–54.

Emanuel, K. A. (1988), The maximum intensity of hurricanes, *J. Atmos. Sci.*, *45*, 1143–1155.

Englehart, P. J., and A. V. Douglas (2001), The role of eastern North Pacific tropical storms in the rainfall climatology of western Mexico, *Int. J. Climatol.*, *21*, 1357–1370.

Ferreira, R. N., and W. H. Schubert (1997), Barotropic aspects of ITCZ breakdown, *J. Atmos. Sci.*, *54*, 261–285.

Fink, A. H., and D. G. Vincent (2003), Tropical cyclone environments over the northeastern Pacific, including mid-level dry air intrusion cases, *Meteorol. Atmos. Phys.*, *84*, 293–315.

Gaffney, S. J., A. W. Robertson, P. Smyth, S. J. Camargo, and M. Ghil (2007), Probabilistic clustering of extratropical cyclones using regression mixture models, *Clim. Dyn.*, *29*, 423–440.

Goddard, L., and M. Dilley (2005), El Niño: Catastrophe or opportunity?, *J. Clim.*, *18*, 651–665.

Goldenberg, S. B., and L. J. Shapiro (1996), Physical mechanisms for the association of El Niño and West African rainfall with Atlantic major hurricane activity, *J. Clim.*, *9*, 1169–1187.

Gray, W. M. (1984), Atlantic seasonal hurricane frequency. Part I: El-Niño and 30-MB quasi-biennial oscillation influences, *Mon. Weather Rev.*, *112*, 1649–1688.

Gray, W. M., and J. D. Sheaffer (1991), El Niño and QBO influences on tropical cyclone activity, in *Teleconnections Linking Worldwide Anomalies*, edited by M. H. Glantz, R. W. Katz, and N. Nicholls, pp. 257–284, Cambridge Univ. Press, New York.

Gray, W. M., C. W. Landsea, P. W. Mielke, Jr., and K. J. Berry (1993), Predicting Atlantic basin seasonal tropical cyclone activity by 1 August, *Weather Forecasting*, *8*, 73–86.

Harr, P. A., and R. L. Elsberry (1995), Large-scale circulation variability over the tropical western North Pacific. Part I: Spatial patterns and tropical cyclone characteristics, *Mon. Weather Rev.*, *123*, 1225–1246.

Hartmann, D. L., and E. D. Maloney (2001), The Madden-Julian oscillation, barotropic dynamics, and North Pacific tropical cyclone formation. Part II: Stochastic barotropic modelling, *J. Atmos. Sci.*, *58*, 2559–2570.

Higgins, R. W., and W. Shi (2005), Relationships between Gulf of California moisture surges and tropical cyclones in the eastern Pacific basin, *J. Clim.*, *18*, 4601–4620.

Irwin, R. P., and R. Davis (1999), The relationship between the Southern Oscillation index and tropical cyclone tracks in the eastern North Pacific, *Geophys. Res. Lett.*, *26*, 2251–2254.

Jáuregui, E. (2003), Climatology of landfalling hurricanes and tropical storms in Mexico, *Atmosfera*, *16*, 193–2004.

Kalnay, E., et al. (1996), The NCEP/NCAR 40-year reanalysis project, *Bull. Am. Meteorol. Soc.*, *77*, 437–441.

Kerr, M. K., and G. A. Churchill (2001), Bootstrapping cluster analysis: Assessing the reliability of conclusions from microarray experiments, *Proc. Natl. Acad. Sci. U. S. A.*, *98*, 8961–8965.

Kimberlain, T. B. (1999), The effects of ENSO on North Pacific and North Atlantic tropical cyclone activity, paper presented at 23rd Conference on Hurricanes and Tropical Meteorology, Am. Meteorol. Soc., Dallas, Tex.

Knaff, J. A. (1997), Implications of summertime sea level pressure anomalies in the tropical Atlantic region, *J. Clim.*, *10*, 789–804.

Knaff, J. A., J. P. Kossin, and M. DeMaria (2003), Annular hurricanes, *Weather Forecasting*, *18*, 204–223.

Landsea, C. W. (2000), El Niño–Southern Oscillation and the seasonal predictability of tropical cyclones, in *El Niño: Impacts of Multiscale Variability on Natural Ecosystems and Society*, edited by H. F. Díaz and V. Markgraf, pp. 149–181, Cambridge Univ. Press, New York.

Landsea, C. W., R. A. Pielke, Jr., A. M. Mestas-Nuñez, and J. A. Knaff (1999), Atlantic basin hurricanes: Indices of climatic changes, *Clim. Change*, *42*, 89–129.

Leith, C. E. (1975), Climate response and fluctuation dissipation, *J. Atmos. Sci.*, *32*, 2022–2026.

Liebmann, B., H. H. Hendon, and J. D. Glick (1994), The relationship between tropical cyclones of the western Pacific and Indian oceans and the Madden-Julian oscillation, *J. Meteorol. Soc. Jpn.*, *72*, 401–411.

Madden, R. A., and P. R. Julian (1972), Description of global circulation cells in the tropics with a 40–45 day period, *J. Atmos. Sci.*, *29*, 1109–1123.

Maloney, E. D., and D. L. Hartmann (2000), Modulation of hurricane activity in the Gulf of Mexico by the Madden-Julian oscillation, *Science*, *287*, 2002–2004.

Maloney, E. D., and D. L. Hartmann (2001), The Madden-Julian oscillation, barotropic dynamics, and North Pacific tropical cyclone formation. Part I: Observations, *J. Atmos. Sci.*, *58*, 2545–2558.

McBride, J. L., and R. Zehr (1981), Observational analysis of tropical cyclone formation. Part II: Comparison of non-developing versus non-developing systems*J. Atmos. Sci.*, *38*, 1132–1151.

Molinari, J., and D. Vollaro (2000), Planetary- and synoptic-scale influences on eastern Pacific cyclogenesis, *Mon. Weather Rev.*, *128*, 3296–3307.

Molinari, J., D. Knight, M. Dickinson, D. Vollaro, and S. Skubis (1997), Potential vorticity, easterly waves, and eastern Pacific tropical cyclogenesis, *Mon. Weather Rev.*, *125*, 2699–2708.

Molinari, J., D. Vollaro, S. Skubis, and M. Dickinson (2000), Origins and mechanisms of eastern Pacific tropical cyclogenesis: A case study, *Mon. Weather Rev.*, *128*, 125–139.

O'Brien, J. J., T. S. Richards, and A. C. Davies (1996), The effect of El Niño on U.S. landfalling hurricanes, *Bull. Am. Meteorol. Soc.*, *77*, 773–774.

Pielke, R. A.Jr., and C. N. Landsea (1999), La Niña, El Niño and Atlantic hurricane damages in the United States, *Bull. Am. Meteorol. Soc.*, *80*, 2027–2033.

Reynolds, R. W., N. A. Rayner, T. M. Smith, D. C. Stokes, and W. Wang (2002), An improved in situ and satellite SST analysis for climate, *J. Clim.*, *15*, 1609–1625.

Romero-Vadillo, E., O. Zaytsev, and R. Morales-Pérez (2007), Tropical cyclone statistics in the northeastern Pacific, *Atmosfera*, *20*, 197–213.

Sánson, L. Z. (2004), The mechanical influence of continental topography on the trajectories of tropical cyclones near the west coast of México, *Atmosfera*, *17*, 151–170.

Shapiro, L. J. (1987), Month-to-month variability of the Atlantic tropical circulation and its relationship to tropical storm formation, *Mon. Weather Rev.*, *115*, 1598–1614.

Smith, S. R., J. Brolley, and C. A. Tartaglione (2007), ENSO's impact on regional U.S. hurricane activity, *J. Clim.*, *20*, 1404–1414.

Tang, B. H., and J. D. Neelin (2004), ENSO influence on Atlantic hurricanes via tropospheric warming, *Geophys. Res. Lett.*, *31*, L24204, doi:10.1029/2004GL021072.

Tartaglione, C. A., S. R. Smith, and J. J. O'Brien (2003), ENSO impact on hurricane landfall probabilites for the Caribbean, *J. Clim.*, *16*, 2925–2931.

Vincent, D. G., and A. H. Fink (2001), Tropical cyclone environments over the northeastern and northwestern Pacific based on ERA-15 analyses, *Mon. Weather Rev.*, *129*, 1928–1948.

Wang, B., and J. C. L. Chan (2002), How strong ENSO events affect tropical storm activity over the western North Pacific, *J. Clim.*, *15*, 1643–1658.

Wheeler, M. C., and H. H. Hendon (2004), An all-season real-time multivariate MJO index: Development of an index for monitoring and prediction, *Mon. Weather Rev.*, *132*, 1917–1932.

Whitney, L. D., and J. Hobgood (1997), The relationship between sea surface temperature and maximum intensities of tropical cyclones in the eastern North Pacific, *J. Clim.*, *10*, 2921–2930.

Wu, P., and P.-S. Chu (2007), Characteristics of tropical cyclone activity over the eastern North Pacific: The extremely active 1992 and the inactive 1977, *Tellus, Ser. A*, *59*, 444–454.

Zehnder, J. A. (1991), The interaction of planetary-scale tropical easterly waves with topography: A mechanism for the initiation of tropical cyclones, *J. Atmos. Sci.*, *48*, 1217–1230.

Zehr, R. M. (1992), Tropical cyclogenesis in the western North Pacific, *NOAA Tech. Rep. NESDIS 61*, 181 pp., NOAA, Washington, D. C.

Zhao, X., and P.-S. Chu (2006), Bayesian multiple changepoint analysis of hurricane activity in the eastern North Pacific: A Markov chain Monte Carlo approach, *J. Clim.*, *19*, 564–578.